

Unilag Journal of Mathematics and Applications,

Volume 5, Issue 1 (2025), Pages 39–50.

ISSN: 2805 3966. URL: http://lagjma.edu.ng

NUMERICAL COMPUTATION OF CHEMICAL REACTION, HEAT GENERATION, THERMAL RADIATION, AND VISCOUS DISSIPATION EFFECTS ON MAGNETOHYDRODYNAMIC (MHD) CONVECTIVE FLOW THROUGH A POROUS MEDIUM

SOLUADE JOSEPH AROLOYE 1, RILWAN OLUWANISHOLA BALOGUN 2, AND AKUDO PAMELA IJEZIE 3

ABSTRACT. This research explores the effect of viscous dissipation on free convection magnetohydrodynamic (MHD) flow through a porous medium over an exponentially stretching surface in the presence of a chemical reaction. The fundamental governing partial differential equations (PDEs) governing the problems are transformed into nonlinear ordinary differential equations (ODEs) using similarity variable. Numerical solutions are then obtained through the shooting method combined six order Runge Kutta Scheme. Maple software is used for the simulation of the problem. The characteristics of boundary layer flow, along with the behaviour near the bounding surface, and the effect of embedded flow parameters on velocity, temperature and concentration profiles are examined and interpreted through graphical illustrations. The findings indicate that an increase in the Eckert number, radiation, and magnetic parameter (M) enhances the temperature profiles, whereas a rise in the chemical reaction parameter, porosity, and Schmidt number reduces the concentration profiles. To ensure accuracy, a comparative analysis between the present results and previously published outcomes for a specific case is performed, revealing strong agreement.

1. Introduction

Engineering and industrial processes, such as extrusion techniques, biological fluid movement, hot rolling, glass-fiber manufacturing, metallic plate cooling, rubber sheet production, lubricant and paint performance, wire drawing, melt-spinning, plastic manufacturing, polymer extrusion, and aerodynamic plastic sheet extrusion, have garnered significant research attention over recent decades

²⁰¹⁰ Mathematics Subject Classification. Primary: 22E30. Secondary: 58J05.

Key words and phrases. Viscous dissipation; Magnetohydrodynamic; Runge Kutta; Stretching Surface; Thermal radiation)

using the 2010 MSC must be included in your manuscript.

^{©2025} Department of Mathematics, University of Lagos.

Submitted: August 8, 2025. Revised: September 9, 2025. Accepted: September 30, 2025.

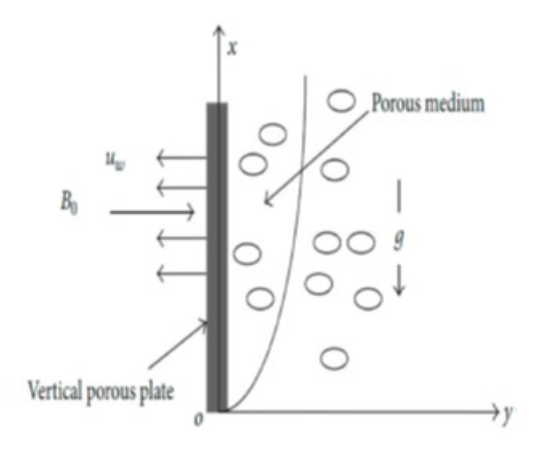
¹ Correspondence.

Table 1. Nomenclature.

A_1 : Constant	S: Source Parameter
B_1 : Constant	(x,y): Cartesian coordinates
B_0 : Coefficient of magnetic field	(x,y): Velocity components along (x,y)-axes
C_p : Specific heat	M: Magnetic Parameter
D: Molecular Diffusivity	
C_R : Chemical reaction Parameter	Greek sybol
K_P : Permeability of the fluid	η : Similarity variable
a: Thermal diffusivity	ϕ : Dimensionless concentration
Q: Dimensional heat source	ρ : Density
q_r : Radiative heat flux	ψ : Stream function
K_p : Rate of chemical reaction	ν Kinematic viscosity θ
$\frac{1}{K_p}$: Porosity parameter	θ Dimensionless temperature
R: Radiation Parameter	Super scripts
k: Thermal conductivity	Differentiation with respect to ρ
μ : Dynamic viscosity of the fluid	
Sc: Schmidt number	Subscripts
Ec: Eckert number	w: Conditions at the wall
Pr: Prandtl number	∞ The outer edge of the boundary layer

to investigate fluid flow over a stretching sheet. Numerous researchers have studied fluid behaviour on such surfaces, [23], [20] and [13]. The impact of thermal radiation on convective fluid flows has widespread applications in physics and engineering, including gas-cooled nuclear reactors, gas turbines, propulsion systems, hypersonic flights, space vehicles, solar power systems, nuclear plants, and various industrial processes. This topic has attracted considerable attention from researchers such as [16], [4] and [17]. The study of magnetohydrodynamic (MHD) flow of electrically conductive fluids is crucial in modern metallurgical and physical processes due to the magnetic field's effect on boundary layer regulation and efficiency in systems utilizing conductive fluids. MHD flow has broad engineering applications and has been extensively researched, [3], [19], [12] including plasma studies, geothermal energy extraction, MHD generators, nuclear reactor safety, and furnace design. Additionally, hydromagnetic methods are applied in purifying molten metals from non-metallic inclusions using magnetic fields. [7] investigated MHD boundary layer flow of nanofluid and heat transfer over a porous exponentially stretching sheet in presence of thermal radiation and chemical reaction with suction. The analysis of heat and mass transfer in fluids over exponentially extending surfaces with chemical reactions plays a vital role in applications such as nuclear reactors, aeronautics, drying processes, cosmic fluid dynamics, heat exchangers, geothermal systems, chemical engineering, construction, solar physics, solar collectors, and oil recovery. Several studies [[6], [5] and [5]] have explored chemical reactions over stretching sheets. [8] examined the viscous dissipation and partial slip effects on mhd boundary layer flow of nanofluid and heat transfer over a nonlinear stretching sheet with non-uniform heat source.

Viscous dissipation refers to the irreversible process where shear forces convert mechanical energy into heat within a fluid. In abnormal flow fields or strong gravitational environments, viscous dissipation characterized by the Eckert number becomes significant in natural convection. For example, [11] analysed the radiative flow of nanofluid from an MHD boundary layer along a vertical plate with a source/sink. [15] examined micropolar nanofluid flow with viscous dissipation and MHD effects past a stretching sheet. [2] studied the impact of Soret, Dufour, Hall current, and rotation on MHD natural convection heat and mass transfer past an accelerated vertical plate in a porous medium. [21] analysed thermal radiation and Joule heating effects on MHD Casson nanofluid flow with chemical reactions through a non-linear inclined porous stretching sheet. [9] investigated heat generation/absorption effects on MHD copper-water nanofluid flow over a non-linear stretching/shrinking sheet. [10] further examined MHD boundary layer nanofluid flow and heat transfer, while [22] discussed unsteady MHD free convective flow past a vertical porous plate with variable suction. Additionally, [1] analysed hydromagnetic free convection heat transfer in Couette flow of water at 4C within a rotating system. Motivated by the aforementioned research and the extensive industrial relevance of this topic, this study aims to explore the combined effects of viscous dissipation, heat generation, thermal radiation, chemical reactions and magnetic effect on MHD free convection flow over an exponentially stretching sheet within a porous medium. This work expands upon the findings of [23] and [18] to address a broader scope, incorporating the influence of multiple flow parameters on MHD behaviour. Numerical solutions are obtained using the Shooting method combined with six order Runge Kutta scheme. Maple software is used for the simulation of the problem. The results obtained are presented through graphical illustrations and tables to highlight the impact of various governing flow parameters.



1.jpg

Fig 1: Flow Geometry

2. Model Formulation

We consider a steady, two-dimensional, laminar, and incompressible natural convective heat and mass transfer along a semi-infinite vertical plate embedded

in a doubly stratified, electrically conducting micropolar fluid. The coordinate system is chosen such that the x-axis aligns with the vertical plate, while the y-axis is perpendicular to it. The physical configuration of the problem is illustrated in Fig. 1. The temperature $T_w(x)$ and species concentration $C_w(x)$ are maintained at the plate. The ambient temperature and concentration are assumed to vary linearly with the vertical distance, expressed as: $T_{\alpha}(x) = T_{\alpha,0} + A_1 x$

 $C_{\alpha}(x) = C_{\alpha,0} + B_1 x \ A_1(x)$ and B1(x) are constants representing the temperature and concentration stratification rates, respectively, and denote the initial ambient temperature $T_{\alpha,0}$ and $C_{\alpha,0}$ concentration at x = 0.

The equations which govern the fluid flow are:

$$\frac{\partial u}{\partial x} + \frac{\partial v}{\partial y} = 0 \tag{2.1}$$

$$u\frac{\partial u}{\partial x} + v\frac{\partial u}{\partial y} = u\frac{\partial^2 u}{\partial x^2} + v\frac{\partial^2 u}{\partial y^2} + -\frac{\sigma B_0^2}{\rho}u - \frac{v}{K_n}u. \tag{2.2}$$

$$u\frac{\partial T}{\partial x} + \frac{\partial T}{\partial y} = \alpha \left(\frac{\partial^2 T}{\partial x^2} + \frac{\partial^2 T}{\partial y^2} \right) - \frac{1}{\rho C_p} \frac{\partial q_r}{\partial y} + \frac{Q}{\rho C_p} (T - T_\infty) + \frac{v}{C_p} \left(\frac{\partial u}{\partial y} \right)^2$$
(2.3)

$$u\frac{\partial C}{\partial x} + v\frac{\partial C}{\partial y} = D\left(\frac{\partial^2 C}{\partial x^2} + \frac{\partial^2 C}{\partial y^2}\right) - k_r\left(C - C_\infty\right). \tag{2.4}$$

where u and v are the components of velocity along coordinate axes, T is the fluid temperature, C is the species concentration. Using the Roseland approximation for radiation, the radiative heat flux q is given by

$$q_r = \frac{-4\sigma^*}{3k^*} - \frac{\partial T^4}{\partial y}. (2.5)$$

Where k^* is the coefficient of mean absorption, σ^* is the Stefan-Boltzman constant. we presume that the temperature difference within the flow adequately small. the expression T^4 , enlarging in a Taylor series in powers of $(T-T^4)$ and neglecting higher-order terms we get

$$T^4 \cong 4T_{\infty}^3 T - 3T_{\infty}^3$$
 Then

$$q_r = \frac{-16\sigma^* T_\infty^3}{3k^*} \frac{\partial T}{\partial y}, \frac{\partial q_r}{\partial y} = \frac{-16\sigma^* T_\infty^3 \partial^2 T}{3\rho C_n k^* \partial y^2}$$
(2.6)

The boundary conditions are

$$u = U_w(x)y = 0, T = T_w, C = C_w, aty = 0$$

$$u \to 0, T \to T_\infty, C \to C_\infty asy \to \infty.$$
 (2.7)

The stream function $\psi(x,y)$ defined by

$$u = \frac{\partial \psi}{\partial y}, v = -\frac{\partial \psi}{\partial x} \tag{2.8}$$

Which satisfies the equation of continuity (1).

Introducing the similarity transformation:

$$\eta = y\sqrt{\frac{u_0}{2vL}}e^{\frac{x}{2L}}, u = u_0e^{\frac{x}{2L}}f'(x), v = -\sqrt{\frac{vu_0}{2vL}}(f(\eta) + \eta f'(\eta))$$

$$T = T_{\infty} + T_0 e^{\frac{x}{2L}} \theta(\eta).C = C_{\infty} + C_0 e^{\frac{x}{2L}} \theta(\eta)$$

$$B = B_0 e^{\frac{x}{2L}} \tag{2.9}$$

Substituting (8) and (9) in (2) - (4), we get

$$f' + ff'' - 2f^2 - \left(M + \frac{1}{K_p}\right)f' = 0 {(2.10)}$$

$$\frac{1}{Pr}\left(1 + \frac{4}{3}R\right)\theta'' + f\theta' - f'\theta + Pr(1 - f')Ec + Ecf'^{2} + S\theta = 0$$
 (2.11)

$$\phi'' + Scf\phi' - Scf'\phi - C_R\phi + (Sc + 1) = 0$$
(2.12)

where

$$Pr = \frac{v}{a}, Sc = \frac{v}{D}, M = \frac{2\sigma B_0^2 L}{\rho u_0 e^{\frac{v}{L}} C_p}, K_p = \frac{K_p' u_0 e^{\frac{v}{L}}}{2Lv}, R = \frac{4\sigma^* T_\infty^3}{K^* K}$$

$$S = \frac{2LQ}{\rho u_0 e^{\frac{v}{L}} C_p}, Ec = \frac{u_w^2}{C_p (T_p - T_\infty)} and C_R = \frac{2LK_R}{U_w}$$

The boundary conditions (7) reduce to the following form:

$$f(\eta) = 0, f'(\eta) = 1, \theta(\eta) = 1at\eta = 0$$

$$f'(\eta) \to 0, \theta(\eta) \to 1, \phi(\eta) \to 1 at \eta = 0$$
 (2.13)

Where η is the similarity variable, $f(\eta)$ is the dimensionless stream function, $\theta(\eta)$ is the dimensionless temperature, $\theta(\eta) = 0$ is the dimensionless concentration, and prime denotes the differentiation with respect to η . Physical Quantities of Interest: Local skin friction coefficient Cf is defined as

$$\frac{1}{sqrt2}C_p\sqrt{R_e} = f^0(0) \tag{2.14}$$

The heat and mass transfers from the plate, respectively, are given by

The field distribution of the place, respectively, the given by
$$q_{w} = -k \left(\frac{\partial T}{\partial y}\right)_{y=0}, q_{m} = -D \left(\frac{\partial C}{\partial y}\right)_{y=0},$$

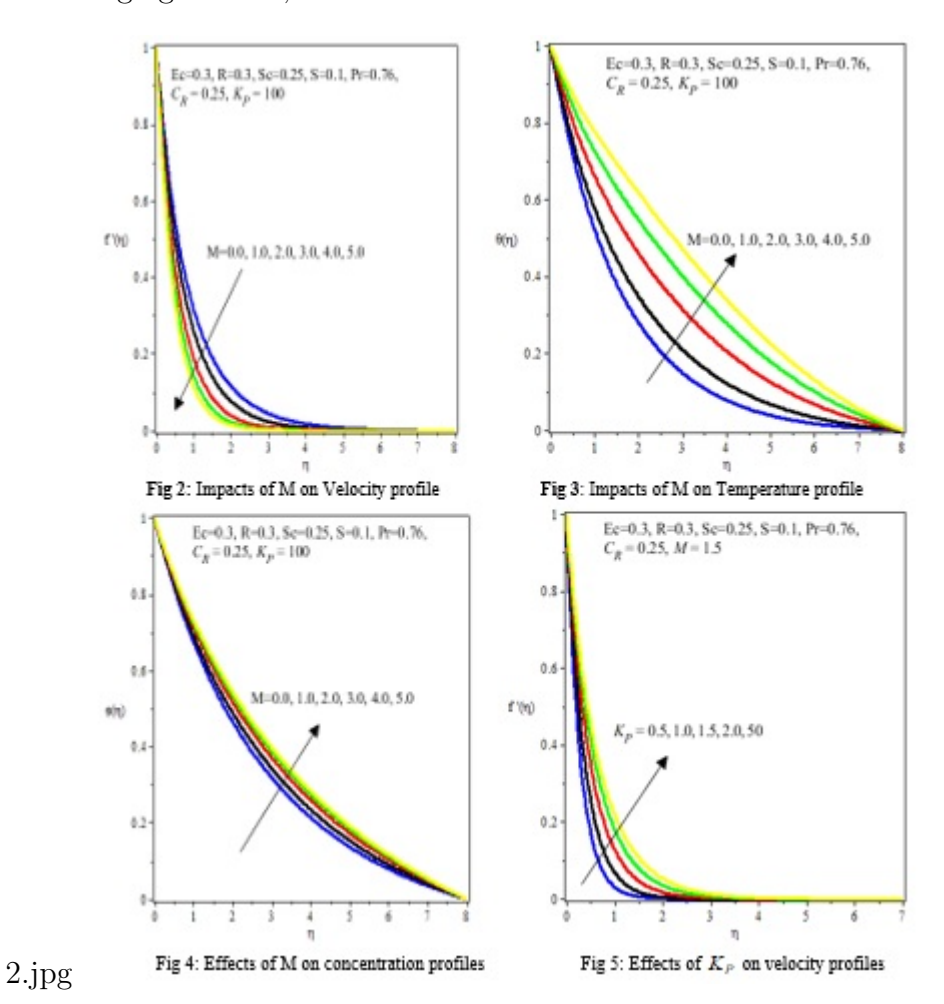
$$\frac{N_{u}}{sqrtR_{e}} = -\theta(0), \frac{S_{h}}{sqrtR_{e}} = -\phi'(0), where R_{e} = \frac{U_{w}}{v}.$$
(2.15)

3. Numerical Solution

The system of coupled system of ordinary differential equations (10), (11), and (12), together with the boundary conditions (13), is numerically solved using the shooting technique, incorporating the sixth-order RungeKutta method across a range of moderate flow, heat, and mass transfer parameters. The Broyden algorithm is applied to refine the initial guesses and ensure the boundary conditions at infinity are met. The numerical simulations are carried out using the Maple software package.

4. RESULT AND DISCUSSION

The velocity, temperature, and concentration profiles for relevant flow parameters are illustrated in Figures 214. Additionally, Tables 13 present the effects of the governing parameters on the skin friction coefficient, Nusselt number, and Sherwood number. A comparative analysis with previously published results has been carried out in Tables1-3 to validate the accuracy of the current findings by comparing our results with previous published result in literature The comparison reveals a strong agreement, as demonstrated in Tables 13.



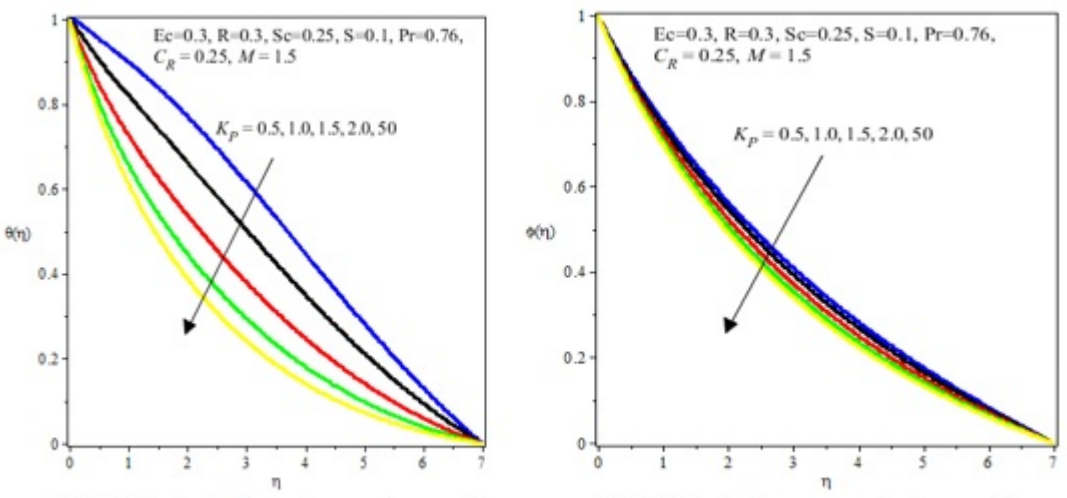
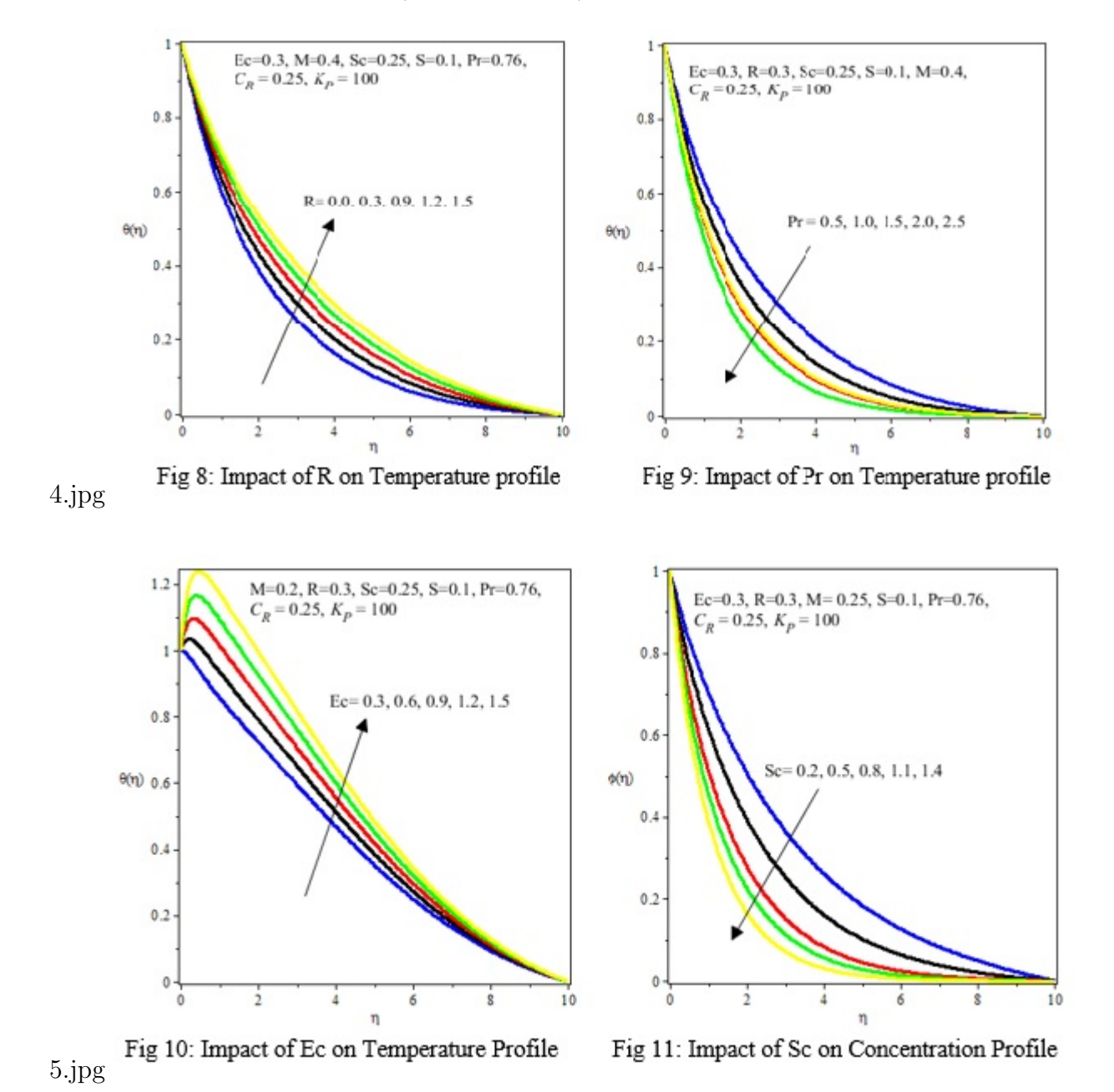


Fig 6: Effects of K_P on temperature profiles

Fig 7: Effects K_P on concentrations profiles

3.jpg

Figure 2 depicts the relationship between velocity and significant of magnetic field values. An increase in M results in a reduction in velocity. As M increases, it generates a resistive force, similar to drag, known as the Lorentz force, which slows down the fluid motion. Figure 3 illustrates the effect of the magnetic field on temperature profiles. It demonstrates that an increase in the magnetic field leads to a rise in the temperature profile. This occurs because the Lorentz force, which is directly linked to the magnetic field, intensifies as the magnetic field strengthens, thereby increasing the temperature. Figure 4 presents the influence of the magnetic field M on dimensionless concentration. The plot indicates that a higher magnetic field M corresponds to an increase in the concentration profile. Figure 5 shows the impact of the porosity parameter K_p on fluid velocity. It is evident that as the porosity parameter increases, the fluid experiences less resistive force, resulting in a higher flow velocity. Figure 6 illustrates the effect of the porosity parameter K_p on temperature profiles. The graph reveals that an increase in K_p causes a reduction in the temperature profile. Figure 7 displays the influence of the



porosity parameter K_p on dimensionless concentration. The plot indicates that as K_p increases, the concentration profile decreases. Figure 8 depicts the effect of radiation R on the temperature profile. An increase in radiation R leads to a rise in temperature, which results from a reduction in the heat transfer rate across the surface region. Figure 9 illustrates how the Prandtl number influences the temperature profile. It is observed that an increase in the Prandtl number reduces the thickness of the thermal boundary layer. Figure 10 demonstrates the effect of the Eckert number Ec on the temperature profile. As the Eckert number Ec increases, a corresponding rise in temperature is observed. Figure 11 highlights the impact of the Schmidt number Sc on the dimensionless concentration. It is

evident that as the Schmidt number Sc increases, the concentration decreases.

2.311634

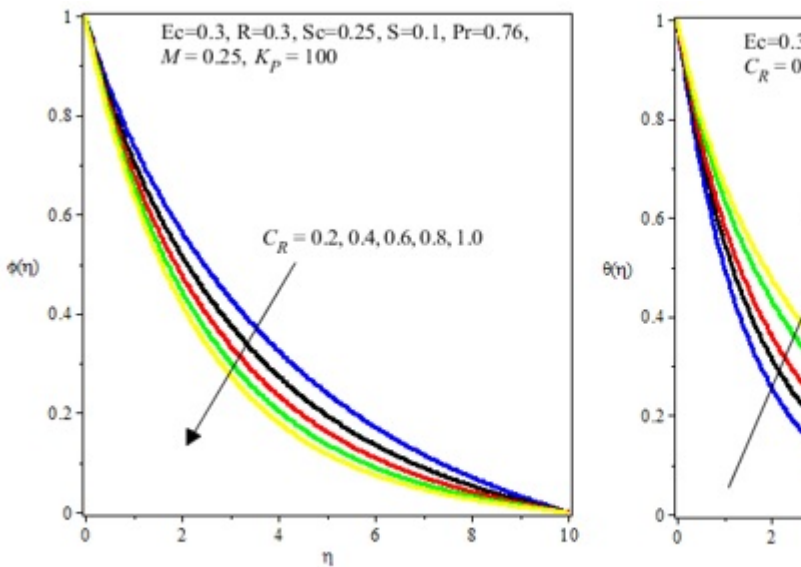
Figure 12 displays the effect of the chemical reaction parameter C_R on the concentration profile. An increase in the chemical reaction parameter C_R results in a reduction in concentration. Figure 13 presents the influence of the source parameter S on the temperature profile. The temperature profile is observed to increase as the source parameter S becomes larger.

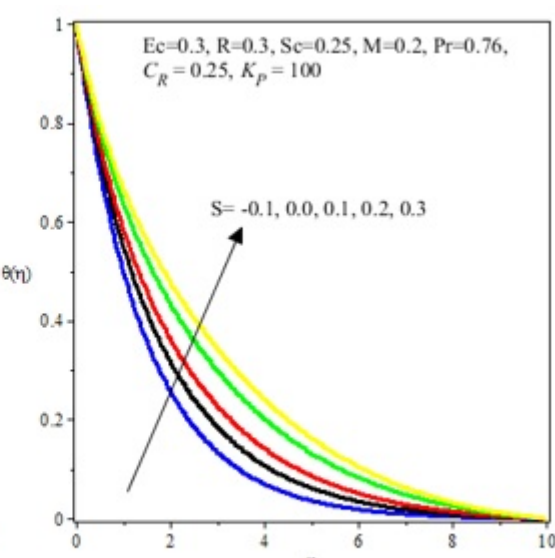
Table 1 outlines the effects of the magnetic field and the porosity parameter on the skin friction coefficient. The results indicate that an increase in the magnetic field strengthens the Lorentz force, thereby raising the skin friction coefficient. Conversely, an increase in the porosity parameter produces an opposite effect, leading to a decrease in the skin friction coefficient.

S	M	K_p	f''(0)	f''(0)	f''(0)	f''(0)
				Swain et al. (2015)	Reddy et al(2021)	Present Result
1	0	100	1.070259	1.079185	1.079185	1.079186
2	1	100	2.698484	2.671235	2.671235	2.671234
3	1	0.5	3.015113	3.012158	3.012158	3.012158

2.311632

TABLE 2. Skin friction coefficient f' value for M and K_p .





2.311632

Fig 12: Effects of C_R on Concentration profile .

100

2.310844

Fig 13: Effect of S on Temperature Profile

6.jpg

4

M	K_p	P_r	R	S	$-\theta(0)$	$-\theta(0)$	$-\theta(0)$
					Swain et al. (2015)	Reddy et al(2021)	Present Result
0	100	1	1	0	0.5311	0.5224	0.5223
0	100	2	1	0	1.4175	1.4065	1.4062
0	100	1	0	0	0.9547	0.9472	0.9471
0	0.5	1	1	0	0.4318	0.4232	0.4231
0	0.5	2	1	0	1.2137	1.2154	0.2154
0	0.5	1	0	0	0.7643	0.7438	0.7439
1	100	1	1	0.1	0.9633	0.9401	0.9402
1	0.5	1	1	0.1	0.7835	0.7528	0.7529

Table 3. Sherwood number $-\theta(0)$ value for M, K_p, P_r, R, S .

Table 4. Sherwood number $-\theta(0)$ value for M, Sc, K_p ,

S	M	Sc	K_p	$-\theta(0)$	$-\theta(0)$	$-\theta(0)$
				Swain et al. (2015)	Reddy et al(2021)	Present Result
1	3	0.6	100	1.331674	1.31175	1.31176
2	3	0.22	0.5	-1.90499	-1.9081	-1.9082
3	3	0.1	0.5	-2.35153	-2.3414	-2.3415
4	4	0.6	0.5	-2.14054	-2.1341	-2.1342
5	4	0.78	0.5	-1.90499	-1.9074	-1.9075

Table 2 presents the influence of Pr, R, and S on the local Nusselt number (Nu). The local Nusselt number increases with a rise in Pr for both $K_p = 100$ and $K_p = 0.5$. When $K_p = 100, Nu$ exhibits a steady increase as the radiation parameter (R) increases. However, for $K_P = 0.5, Nu$ decreases as the radiation parameter increases. Additionally, at $K_p = 0.5$, the local Nusselt number increases with a rise in the source parameter (S) due to greater heat energy accumulation. Table 3 displays the Sherwood number (Sh) values based on variations in the magnetic parameter (M) and the Schmidt number (Sc). The table reveals that the Sherwood number decreases as the magnetic parameter increases, whereas it increases when the Schmidt number rises.

5. Conclusion

The influence of certain governing parameters was analysed and presented through graphical illustrations, revealing that an increase in the magnetic field strength reduces the dimensionless velocity while enhancing both the nanoparticle concentration and dimensionless temperature, while a rise in the porosity parameter leads to an increase in the velocity profile, with a decreasing trend observed in the concentration and temperature fields. Additionally, a higher Prandtl number results in a reduction of the temperature profile, and an increase in temperature corresponds to a rise in the Eckert number, radiation parameter, and heat source parameter, whereas larger values of the Schmidt number and the chemical reaction parameter lead to a reduction in nanoparticle concentration.

5.1. **Acknowledgement.** The author would like to thank the Isaac Newton Institute for Mathematical Sciences, United Kingdom for support and hospitality during the programme [Modern History of Mathematics] where work on this paper was undertaken. This work was supported by EPSRC grant no EP/K032208/1

References

- Anand Rao R Srinivasa Raju, J., Jithender Reddy, G., Dharmendar Reddy, Y., Anand Rao, J. Hydromagnetic free convection heat transfer Couette flow of water at 40C in rotating system, Proceedings of International Conference on Mathematical Computer Engineering-(ICMCE-2015) 978-993. 2015
- [2] Anil Kumar, M., Dharmendar Reddy, Y., Shankar Goud, B., Srinivasa Rao, V. Effects of soret, dufour, hall current and rotation on MHD natural convective heat and mass transfer flow past an accelerated vertical plate through a porous medium, International Journal of thermo fluids, International Journal of Thermofluids 9 100061, 2021
- [3] AnilKumar, M., Dharmendar Reddy, Y., Srinivasa Rao, V., ShankarGoud, B. Thermal radiation impact on MHD heat transfer natural convective nano fluid flow over an impulsively started vertical plate, Case Studies in Thermal Engineering 24, 100826. 2021.
- [4] Asha, S.K. and Sunitha, G. Thermal radiation and Hall effects on peristaltic blood flow with double diffusion in the presence of nanoparticles, Case Studies in Thermal Engineering 17 100560. 2020
- [5] Bhowmik, H., Gharibia, A., Yaarubia, A., Alawia, N. (2019). Transient natural convection heat transfer analyses from a horizontal cylinder, Case Studies in Thermal Engineering 14 100422, 2019.
- [6] Chunquan Li, Jian Huang, Yuling Shang, Hongyan Huang, Study on the flow and heat dissipation of water-based alumina nanofluids in microchannels, Case Studies in Thermal Engineering 22 100746, 2020.
- [7] Dharmendar Reddy, Y., Srinivasa Rao, V. and Anand Babu, L. MHD boundary layer flow of nanofluid and heat transfer over a porous exponentially stretching sheet in presence of thermal radiation and chemical reaction with suction, Int. J. Math. Trends Technol. 47 (2). 2017a.
- [8] Dharmendar Reddy, Y., Srinivasa Rao, V., Anand Babu, L. Viscous dissipation and partial slip effects on mhd boundary layer flow of nanofluid and heat transfer over A nonlinear stretching sheet with non-uniform heat source, International Journal of Mathematical Archive 8 (8). EISSN 2229-5046. 2017b.
- [9] Dharmender Reddy, Y. Srinivasa Rao, V., Anil Kumar, M., Effect of heat generation/absorption on MHD copper-water nanofluid flow over a non-linear stretching/shrinking sheet, AIP Conference Proceedings 2246 (2020), 020017. 2020.
- [10] Dharmender Reddy, Y., Srinivas Rao, V., Babu Ramya, D., Anand, L. MHD boundary layer flow of nanofluid and heat transfer over a nonlinear stretching sheet with chemical reaction and suction/blowing, Journal of Nanofluids 7 (2), 404412, 9. 2018.
- [11] Ganga, B., Mohamed Yusuff Ansari, S., Vishnu Ganesh, N., Abdul Hakeem, A.K. MHD radiative boundary layer flow of nanofluid past a vertical plate with internal heat generation/absorption, viscous and ohmic dissipation effects, Journal of the Nigerian Mathematical Society 34 (2015) 181194.
- [12] Idowu, A.S. and Falodun, B.O. SoretDufour effects on MHD heat and mass transfer of Walters-B viscoelastic fluid over a semi-infinite vertical plate: spectral relaxation analysis, Journal of Taibah University for Science 13 4962. (2019).
- [13] Iswar Chandra Mandal, Swati Mukhopadhyay, Heat transfer analysis for fluid flow over an exponentially stretching porous sheet with surface heat flux in a porous medium, Ain Shams Engineering Journal 4 (2013) 103110.

- [14] Jena, S. Dash, G.C., and Mishra, S.R. Chemical reaction effect on MHD viscoelastic fluid flow over a vertical stretching sheet with heat source/sink, Ain Shams Engineering Journal 9, 12051213. (2018).
- [15] Kai-Long Hsiao, Micropolar nanofluid flow with MHD and viscous dissipation effects towards a stretching sheet with multimedia feature, Int. J. Heat Mass Tran. 112, 983990. (2017).
- [16] Kalpna Sharma, Sumit Gupta. Analytical study of MHD boundary layer flow and heat transfer towards a porous exponentially stretching sheet in presence of thermal radiation, Int. J. Adv. Appl. Math. Mech. 4 (1). 110, 4(1). (2016).
- [17] Mishra, S.R., Mohammad Mainul Hoque, Mohanty, B., Anika, N.N. Heat transfer effect on MHD flow of a micropolar fluid through porous medium with uniform heat source and radiation, Nonlinear Eng. 8, 6573. (2019).
- [18] Reddy, N.N., Rao, V.S., and Reddy, B.R., Chemical reaction impact on MHD natural convection flow through porous medium past an exponentially stretching sheet in presence of heat source/sink and viscous dissipation. Case Studies in Thermal Engineering 25 (2021) 100879 (2021).
- [19] Rout, B.C. and Mishra, S.R. Thermal energy transport on MHD nanofluid flow over a stretching surface, Engineering Science and Technology, Int. J. 21 6069. (2018).
- [20] Samir kumar Nandy, Tapas Ray Mahapatra, Effects of slip and heat generation/absorption on MHD stagnation flow of nanofluid past a stretching/shrinking surface with convective boundary conditions, Int. J. Heat Mass Tran. 64 (2013) 10911100.
- [21] Shankar Goud, B., Dharmendar Reddy, Y. Srinivasa Rao, V. and Zafar Hayat Khan, Thermal radiation and Joule heating effects on a magnetohydrodynamic Casson nanofluid flow in the presence of chemical reaction through a non-linear inclined porous stretching sheet, J. Nav. Architect. Mar. Eng. 17, 143164. (2020).
- [22] Srinivasa Raju, R., Anil Kumar, M., and Dharmendar Reddy, Y. Unsteady MHD free convective flow past a vertical porous plate with variable suction 11 (23) 1360813616. (2016).
- [23] Swain, I., Mishra, S.R., Pattanayak, H.B. Flow over exponentially stretching sheet through porous medium with heat source/sink, J. Eng. 7. Article ID 452592. (2015).
- [24] Yanala Dharmendar Reddy, Dodda Ramya, Laxmianarayanagari Anand Babu, Effect of thermal radiation on MHD boundary layer flow of nanofluid and heat transfer over a non-linearly stretching sheet with transpiration, Journal of Nanofluids 5 (6), 889897, 9. (2016).

Soluade Joseph Aroloye ¹

DEPARTMENT OF MATHEMATICS, UNIVERSITY OF LAGOS, AKOKA, LAGOS STATE, NIGERIA. E-mail address: saroloye@unilag.edu.ng

RILWAN OLUWANISHOLA BALOGUN 2

Basic Science Unit, School of Science and Technology, Pan-Atlantic University, Lagos.

Akudo Pamela Ijezie

Basic Science Unit, School of Science and Technology, Pan-Atlantic University, Lagos.